

# Intelligent thermochromic heating e-textile for personalized temperature control in healthcare

Ching Lee<sup>1,2</sup>, Jeanne Tan<sup>1,2\*</sup>, Jun Jong Tan<sup>2</sup>, Hiu Ting Tang<sup>1,2</sup>, Wing Shan Yu<sup>2</sup> and Ngan Yi Kitty Lam<sup>1</sup>

<sup>1</sup>School of Fashion and Textiles, The Hong Kong Polytechnic University, Hung Hom, Hong Kong Special Administrative Region.

<sup>2</sup>Laboratory for Artificial Intelligence in Design, Hong Kong Science Park, New Territories, Hong Kong Special Administrative Region.

\*Corresponding Author. Email: [jeanne.tan@polyu.edu.hk](mailto:jeanne.tan@polyu.edu.hk)

## Abstract

Heating electronic textiles (E-textiles) are widely used for thermal comfort and energy conservation, but prolonged heating raises concerns about heat-related illnesses, especially in the elderly. Despite advancements, achieving universal user satisfaction remains difficult due to diverse thermal needs. This paper introduces an intelligent thermochromic heating e-textile with an artificial intelligence (AI)-based temperature control system for optimized personal comfort and colour indicators for elderly caregivers. The fabric integrates conductive yarn, temperature-induced discoloration yarn (TIDY), and polymeric optical fiber (POF) to visualize temperature changes, ensuring efficiency and comfort. Equipped with microcontrollers, ambient sensors, and Bluetooth connectivity, it offers comprehensive intelligent heating solutions. An AI model, trained on data from 50 wearability test subjects, determines optimal heating temperatures (40-50°C) with

5.083 Mean Squared Error (MSE), showing a high correlation between predicted and actual comfort levels. This concept enhances thermal comfort and mitigates overheating risks, promising for wearable healthcare applications.

Keywords: intelligent textile, heating textile, temperature control, thermochromic textile and healthcare

### **Teaser**

An AI-driven thermochromic e-textile optimizes thermal comfort and safety with colour-changing indicators and intelligent heating control.

## **INTRODUCTION**

Heating electronic textiles (E-textiles) are widely applied in sustaining the fundamental physiological well-being of individuals, alongside safeguarding against cold-induced injuries and ailments. The emergence of e-textiles as flexible heaters, integrating electronic components with conductive carbon fibers or silver-coated polymeric yarns,<sup>1-5</sup> offering a diverse range of applications spanning industries such as automotive, healthcare, sports, and domestic use, commonly in form of heating pads,<sup>6-8</sup> shoulder pads,<sup>9</sup> heated mattresses,<sup>10</sup> as well as in form of wearable such as thermal underwear, scarves,<sup>11</sup> and garments.<sup>12</sup> Textile-based temperature sensors and thermally responsive actuators are consistently integrated to monitor the wearer's physiology and environmental changes, thus creating a customized thermal environment. This type of wearable system, known as Personal Thermal Comfort System (PTCS), effectively shifts temperature control from the built environment to the microclimate surrounding the body through wearable textiles.<sup>13</sup> This approach ensures human body healthcare while promoting energy saving.

Temperature control in the intelligent e-textiles are commonly integrate with a diverse array of functional sensors, such as human body sensors,<sup>6</sup> heart rate sensors, blood pressure sensors, and even gesture recognition sensors for regulating the temperature level of the heating e-textiles based on the instant changes of human body.<sup>10</sup> Temperature adjustors, controllers,<sup>14</sup> thermocouples/thermostats,<sup>15, 16</sup> and over-temperature alarm protection devices are commonly in cooperate in use for temperature control.<sup>7</sup> However, despite the promising advanced technology offered by current heated textile wearables in adjusting temperature levels via mobile app control by Bluetooth, manually controlled heated textiles still pose risks of heat-related illness, leading to low-temperature burns during prolonged exposure to skin temperatures of about 44 to 50°C. Several concerns have arisen regarding physical or psychological discomfort, as well as the life-threatening risks of hyperthermia exceeding 37.3 to 38.5°C or hypothermia below 35.0°C when these thermal e-textiles adhere closely to the human skin with uncontrolled temperature fluctuations during extended wear.<sup>17</sup> Regarding to elderly care, due to a decrease in thermosensitivity, the elderly may inadvertently suffer heat burns during prolonged usage. This is a key reason why elderly caregivers often refrain from allowing the elderly to use heating e-textiles. In traditional elderly care centers in Hong Kong, staffing ratios in various care homes are inconsistent, with one staff member taking care of 35 elderly residents in some places.<sup>18</sup> In 2022, the care home industry, which currently employs around 45,000 people, has a vacancy rate of nearly 20%. The current workforce of 45,000 represents only 80% of the required staff, meaning the industry is short of 20%, or 11,250 workers.<sup>19</sup> In certain elderly care centers, elderly individuals are forbidden to use heating pads for cold prevention due to the uncontrollable heating temperature of the pads and the delayed heat sensation of elderly skin, which may lead to easily occurring heat burns.<sup>20, 21</sup> Furthermore, caregivers often lack sufficient time and effective methods to monitor each elderly individual's usage of heating e-textiles. This limitation contributes to the restricted

usage of heating e-textiles in elderly care. As a result, one innovation in this study is the creation of flexible, large-area temperature-induced indicators for caregivers to easily monitor elderly individuals' usage of heating e-textiles, thereby increasing the likelihood of elderly individuals utilizing heating e-textiles without posing a risk of burns.

Thermochromic and illuminative textiles have previously been introduced in both aesthetic and functional textile design. A reversible coloration effect can be achieved in thermochromic textiles by altering the surrounding temperature or exposure to direct sunlight. Common textile products such as T-shirts and caps can be readily fabricated using techniques like knitting, weaving, or embroidering with temperature-induced discoloration yarn (TIDY).<sup>22</sup> Despite this unique ability to change colour across the entire fabric upon heating, which presents great potential in temperature control for smart textile applications, it has rarely been employed in heating textiles before. Polymeric optical fiber (POF) is another textile materials with coloration effect but in dim environment. It has been utilized to achieve illumination through various textile fabrication methods due to its flexibility, lightweight nature, and light-emitting capabilities. The authors possess research expertise in developing interactive POF textiles using woven and knitted structures for applications in fashion, interior design, and sensory environments.<sup>23-25</sup> An artificial intelligence (AI) knitted illuminative textile system was introduced in the past years for multi-sensory stimulation for dementia via gesture recognition.<sup>26, 27</sup> This user-textiles interaction demonstrates the potential application of POF in elderly healthcare and rehabilitation in the future.

Human thermal comfort serves as the principal criterion for evaluating the effectiveness of personal temperature control systems using heating e-textiles in healthcare applications. A systematic review and meta-analysis were conducted to assess the efficacy of conventional heating e-textiles in ensuring human thermal comfort.<sup>28</sup> The findings revealed significant impacts on changes in mean skin temperature, thermal perception, and comfort perception, particularly when

heating the upper torso ( $p < 0.05$ ). Notably, males exhibited higher local skin temperatures than females in cold ambient settings when utilizing e-textiles for heating purposes. These results emphasize the importance of personalized and gender-specific designs for heating e-textiles, which could be further enhanced through the integration of AI to predict thermal comfort across different ages and genders in heating e-textile applications. In a previous study, a machine-learning-based model was proposed to predict thermal comfort recognition in vehicles using user experience-related assessments.<sup>29</sup> The model achieved a thermal comfort prediction by implementing the Long Short-Term Memory (LSTM) model and dataset labels rated on a seven-point scale. This demonstrates the significant potential of employing AI prediction models to examine and differentiate heating temperatures for wearers of varying ages and genders, thus maximizing thermal comfort when using heating e-textiles. A preliminary study proposed a design approach to optimize thermal comfort in electric heating textiles using AI, considering user preferences related to age and gender differences. A fuzzy logic model was established as a proof of concept for temperature regulation by varying ambient temperature, followed by the development of an artificial neural network (ANN) model to predict the optimal temperature for maximum comfort. Results from the ANN model showed promising temperature predictions, while subject tests revealed significant differences in skin temperatures based on gender.<sup>30</sup>

This study introduces an intelligent thermochromic heating jacket (ITHJ) that combines excellent flexibility, temperature-induced colour change, and intelligent temperature control. Unlike traditional PTCS textiles, this innovative textile utilizes an intelligent temperature control system to optimize personal thermal comfort across different age, gender, weight and height of the users. Additionally, it provides vivid temperature-induced colour indicators, aided by TIDY and POF, which is particularly beneficial for elderly caregivers. The fabrication process of ITHJ is simplified, involving the weaving and embroidering of TIDY and POF with conductive yarn to

visualize temperature changes across the fabric surface to form a novel woven illuminative heating fabric (WIHF). This serves as a notification to users and caregivers regarding prolonged heating duration, with superior brightness in both lit and dark environments. Despite the integration of TIDY and POF, this textile retains a great hand feel, offering softness, flexibility, elasticity, smoothness, and breathability. Equipped with thermocouples, heating modules, microcontrollers, ambient sensors for temperature, relative humidity, and air velocity, as well as Bluetooth connectivity, ITHJ provides comprehensive intelligent heating solutions. It includes a trained ANN model in temperature control to predict and regulate optimal heating temperatures, ensuring superior human thermal comfort across various age groups, genders, weights and heights. The ANN model with 5.083 Mean Squared Error (MSE) was trained by data from 50 wearability test subjects determines optimal heating temperatures between 40 and 50°C to achieve maximum thermal comfort. Remarkable temperature control ability is demonstrated by a high correlation between predicted and actual human thermal comfort.

## **RESULTS AND DISCUSSION**

### **Fabrication of ITHJ**

As conceptually shown in the schematic of Fig. 1a, ITHJ integrates several lightweight ambient sensors and microcontrollers with wireless Bluetooth connection, as well as a user-based AI controlling system, to maintain maximum personal thermal comfort. Additionally, the vivid temperature-induced colorant fabric serves as a multifunctional heating textile for healthcare applications. Real-time data-driven ambient parameters, including temperature, relative humidity, and air velocity, are crucial for temperature control during the application of PTCS in different situations.<sup>31-34</sup> Traditional heating e-textiles typically consist of a bunch of wires for connections, leading to discomfort for wearers.<sup>35-37</sup> To eliminate this drawback, a lightweight wireless integrated

ambient sensor is presented. User variation, including gender, age, weight, and height, is another crucial parameter considered in this study, as it influences the thermal sensation of PTCS applications, as indicated by previous studies.<sup>38, 39</sup> To achieve intelligent temperature control of heating e-textiles regardless of user variation, the aforementioned parameters are collected from 50 wearability test subjects during the experiment to record the heating temperature required to reach maximum thermal comfort with the invention of ITHJ. These data are then applied in AI model training to predict the most suitable heating temperature for various wearers to achieve maximum thermal comfort in applying ITHJ. The details will be discussed further in the following sections.

Fig. 1b illustrates the main fabrication procedure and weaving structure of WIHF. To ensure lightweight, flexibility, softness, and comfort of the multifunctional fabric, conductive silver-coated yarn is used instead of carbon fiber in this case to generate heat.<sup>39-41</sup> Additionally, due to the advantages of cotton in comfort and breathability, a commercial cotton yarn is chosen as the flexible substrate in the warp direction during the weaving process.<sup>42, 43</sup> To achieve the desired coloration and illumination effects without sacrificing the fabric's handle, TIDY and POF are woven with a silver-coated conductive heating yarn with an electrical resistance of  $32\Omega/\text{cm}$  in the weft direction. This is followed by the facile embroidering of another silver-coated conductive yarn with an electrical resistance of  $2.54\Omega/\text{cm}$  in the warp direction to form a pair of electrodes that function as the bus bar to complete the electric circuit. Typically, most mature commercial heating e-textile products are constructed using a knitted structure instead of woven.<sup>44, 45</sup> In the traditional manufacturing process of thermal woven fabric, heating materials are woven into the weft direction, interlacing with passive warp yarns. Therefore, the preparation process is time-consuming to substitute multiple passive warp yarns with conductive yarns to establish a pair of electrodes. This may also be a contributing factor to the limited availability of thermal woven

textile products in the market. However, the woven structure is still valued as it consumes less energy compared to the knitted structure.<sup>46</sup> Hence, the embroidering process proposed in this study replaces the time-consuming method of preparing multiple passive warp yarns with conductive yarns for establishing electrodes. In this study, a double-sided structure is adopted in the weaving process to create a large, soft, and comfortable surface of cotton towards the human skin on the technical face side, and a long-floated weft yarn is used for the purpose of vivid colour indication on the technical back side. Microstructures of raw functional materials, including silver-coated conductive yarns in weaving and embroidering, TIDY and POF, as well as microscopic views of the fabric surface, are captured by scanning electron microscopy (SEM) and microscope (Fig. S1)

The integration of TIDY and POF demonstrates superior brightness in both lit and dark environment, serving as a notification to users and caregivers regarding the extended duration of heating (Fig. 1c). A large area of temperature-induced indicators on flexible heating e-textiles is crucial in elderly healthcare.<sup>47-52</sup> Noticeable colour changes are observed in both lit and dark environments. In a lit environment, TIDY transitions from pale purple to hot pink at 30°C, while in a dark environment, programmed electronic components cause POF to change from blue to yellow to red as the temperature increases from 30°C to above 40°C across the entire fabric surface. This vivid colour change is beneficial in elderly healthcare when applying heating e-textiles. Additionally, this functional fabric offers excellent tactile qualities in terms of softness, flexibility, elasticity, smoothness, and breathability, even when integrated with TIDY and POF.

A preliminary temperature control test was conducted before the wearability test involving 50 subjects to ensure that the heating temperature of the jacket could be stably controlled by the integrated microcontroller. Power consumption for heat emission can be adjusted in real-time by the microcontroller based on the temperature sensor's readings, enabling temperature regulation of ITHJ. In Fig. 1d, the results demonstrate stable heating temperatures on the fabric surface despite

changes in ambient temperature, with conditions set at two conditions: Simulated conditions included strong wind (fan on) with an ambient temperature of  $21\pm 1^{\circ}\text{C}$ ,  $60\pm 5\%$  humidity, and 3 m/s air velocity (case 1); and no wind (fan off) with an ambient temperature of  $17\pm 1^{\circ}\text{C}$ ,  $70\pm 5\%$  humidity, and 0.1 m/s air velocity (case 2). The ideal scenario involves increasing the temperature by  $1^{\circ}\text{C}$  per minute from  $30^{\circ}\text{C}$  to  $50^{\circ}\text{C}$  over 20 minutes, during which the heating temperature was well-controlled in both cases. Fig. 1e depicts the ANN model established in this study. Input variables include subjects' information: (1) age, (2) gender, (3) weight, and (4) height, as well as ambient parameters: (5) temperature ( $^{\circ}\text{C}$ ), (6) relative humidity (%RH), and (7) air velocity (m/s). These inputs are used to predict the target output variable—the heating temperature ( $^{\circ}\text{C}$ ) of the ITHJ to achieve maximum thermal comfort.

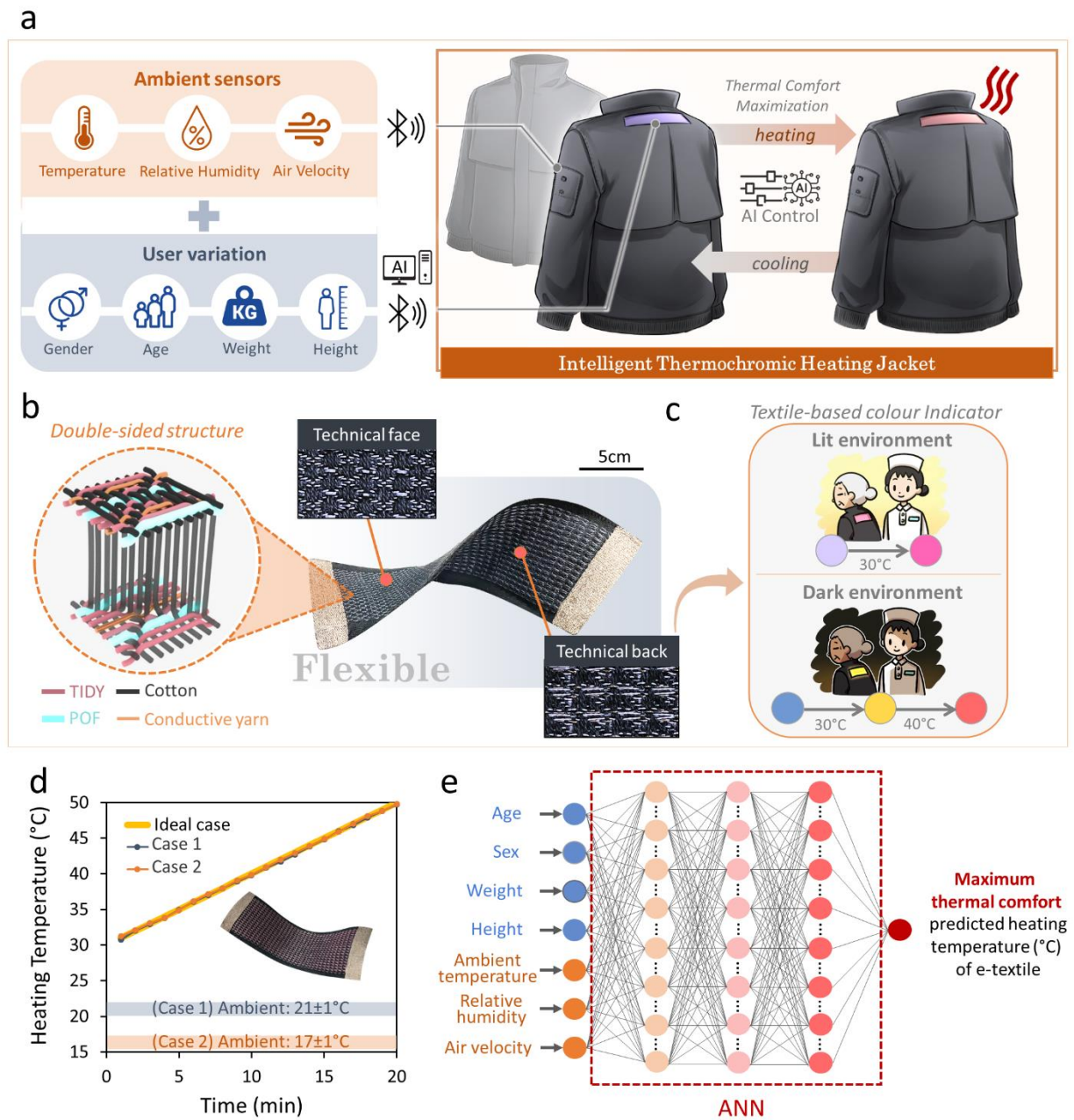


**Fig. 1.** Fabrication of ITHJ. (a) Schematic illustration demonstrates the conceptual design. (b) Fabrication weaving structure. (c) Colouring application in elderly care. (d) Increasing temperature of heating e-textile under ambient temperature, case 1 and case 2 in 20 minutes. (e) Structure of the ANN model in predicting heating temperature of e-textile to achieve maximum thermal comfort.

## Heating Efficiency

It is crucial to have a pair of electrodes connected discreetly with electronic wires to the power supply. In this design, advanced power connection is achieved using removable button clips for both cathode and anode on the embroidering electrodes instead of traditional soldiering.<sup>40</sup> It provides a simple and convenient user-centered approach for daily life applications. This detachable design allows for flexibility in the usage of WIHF. Fig. 2a illustrates the detailed working principle of the temperature control system of WIHF.

The first development of WIHF was proposed recently.<sup>53</sup> Addressing the challenges associated with integrating POF and TIDY without sacrificing heating efficiency, the weft density emerges as a critical factor in maintaining good heating performance of WIHF. Table S1 displays three types of WIHF woven with varying weft density in POF, heating yarn, and TIDY, while keeping the warp density constant. S1 features the loosest weaving structure, whereas S3 has the tightest one. According to previous studies on woven heating e-textiles, it has been observed that heating efficiency enhances as the weft density increases.<sup>54</sup> Results indicated that S3 exhibited the highest current and lowest resistance (Fig. S2). During a 60-minute test under an ambient temperature of 24°C (Fig. 2b), S3 exhibited an initial electrical resistance of 13  $\Omega$  and demonstrated exceptional heating efficiency, reaching 55°C in just 5 minutes, while S1 and S2 remained below 50°C. After 20 minutes heating performance test in this study, the surface heating temperature stabilized at around 50°C for S1, 55°C for S2, and 70°C for S3. Detailed heating performance also showed consistent heating across different power supply levels (5V, 7.5V, 10V, and 12V) (Fig. S3). Fig. 2c displays the average surface heating temperature and current generated from powering fabrics S1, S2, and S3 at 5V, 7.5V, and 12V, respectively. As anticipated, fabric S3 exhibited the highest current and superior heating efficiency, reaching up to 50°C at 12V, with minimal difference

observed at 5V and 7.5V. Fig. 2d illustrates that S3 boasted the highest power density and fabric surface heating temperature among the three fabrics. These results indicate that S3 outperformed the other fabrics in terms of heating performance. To further assess the stability of heating performance for S3, a step test was conducted by incrementally increasing or decreasing power consumption at intervals of 5 minutes for 5V, 7.5V, 10V, and 12V, respectively (Fig. 2e). The figure clearly illustrates that the heating temperature remained well-controlled at 28°C (5V), 33°C (7.5V), 40°C (10V), and 46°C (12V) under an ambient temperature of 24°C, both in ascending and descending order. Fig. 2f demonstrates a stable heating temperature after a 1.5-hour duration in a 10-hour long-run test. The mean surface temperature was recorded by averaging three positions (left, middle, and right) on fabric S3 using a thermal imager. The results indicate an evenly distributed heating temperature on fabric S3, reaching 47°C in 1 minute, 52°C in 5 hours, and 53°C in 10 hours.

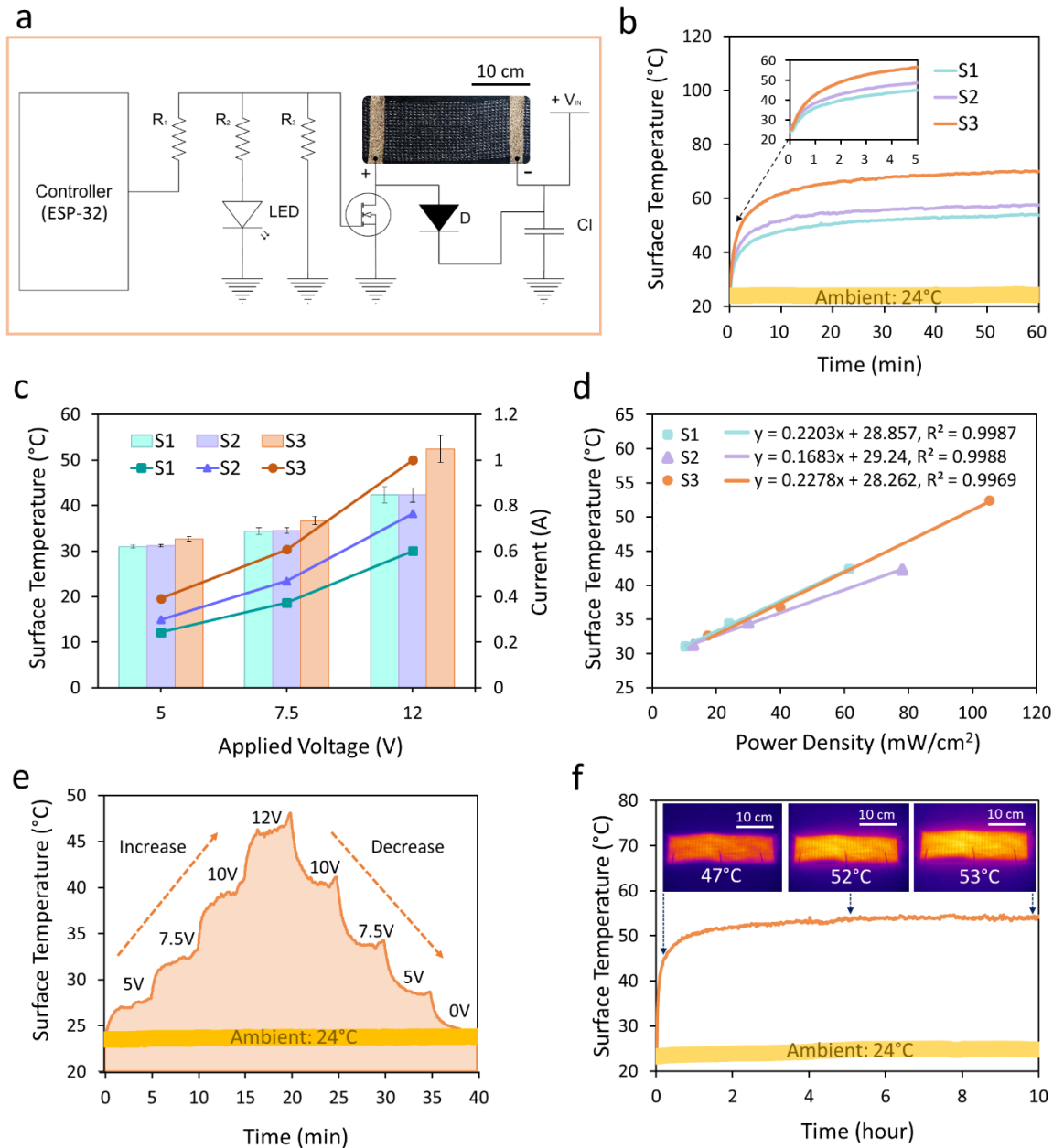


Fig. 2. Design and heating efficiency of WIHF. (a) Schematic illustration of temperature controlling system. (b) Heating temperature of fabric S1, S2 and S3 in 60 minutes test. (c) Heating temperature and current generated from powering fabric S1, S2 and S3 in 5V, 7.5V and 12V respectively. (d) Correlation between power density and heating temperature of fabric S1, S2 and S3. (e) Stability test of fabric S3 by increasing/ decreasing power consumption in 5V, 7.5V, 10 V and 12V per 5 minutes respectively. (f) 10 hours long-run test of fabric S3.

## **Illuminative Performances**

Following the examination of the heating efficacy of the illuminative heating fabric, the temperature-induced colour change and illuminative performance were investigated. While temperature-induced coloured yarn and optical fiber have existed in the textile market for decades, their limited application in heating textile integration has been observed. Therefore, in this study, TIDY and POF were utilized for temperature indication in terms of visual feedback without affecting the heating performance of the fabric. Fig. 3a and 3b illustrate the colour change on the fabric surface when heated to different temperature levels in both lit and dark environments, while observing TIDY and POF, respectively. This novel invention is particularly beneficial in elderly care for caregivers who are responsible for caring for several elderly individuals in daily life. In a lit environment, TIDY demonstrates a pale purple colour when the ambient temperature is below 30°C. Upon powering on the flexible heating textile, the temperature of the fabric surface gradually increases and exceeds 30°C. Consequently, the fabric surface changes from pale purple to hot pink, providing users with a notification of the heating status. It also offers caregivers a visual indication of prolonged heating during elderly usage. In a dark environment, the colour change in TIDY becomes difficult to observe. The illuminative colour on the fabric surface appears blue (R=0, G=0, B=255) when the embedded thermocouple on the fabric surface senses a temperature below 30°C. The colour then gradually changes in a fading mode to yellow (R=255, G=255, B=0) at 40°C and then to red (R=255, G=0, B=0) at 50°C. The function of POF in a dark environment is similar to TIDY in a lit environment, providing alerts for caregivers and users regarding heating textile usage in daily life. Fig. 3c and 3d show images of the colour -changing effect of TIDY and POF on the fabric surface in lit and dark environments, respectively. (Movie S1)

To investigate the gradient of colour change in TIDY, a colour eye spectrophotometer was used

to study reflectance at different power voltage supplies. Fig. 3e demonstrates the colour spectrum of TIDY at 0V, 4.5V, 5V, 5.5V, 6V, and 6.5V between wavelengths of 400 to 700nm. The results show an obvious colour change from purple to pink at 5V, while the pink colour becomes richer and more saturated at 6.5V. In the case of POF, a spectrofluorometer was used to evaluate the fluorescence intensity of blue, yellow, and red illuminated colour. The results in Fig. 3f show distinctive peaks at 420nm, 540nm, and 590nm, corresponding to blue, yellow, and red, respectively. Detailed information on excitation and emission wavelengths is indicated in table S2. The programmed colour change in POF in textile application is intuitive, but limited research has been found in the past. Thus, smart heating e-textiles with TIDY and POF are highly desirable for advanced thermal e-textile technology due to their conspicuous alteration in coloration and illumination, serving the purpose of alerting users to the activation of the textile's heating function, thereby acting as a visual indicator of its ongoing operation. The colour change could also serve as a notification to users and caregivers regarding the extended duration of heating.

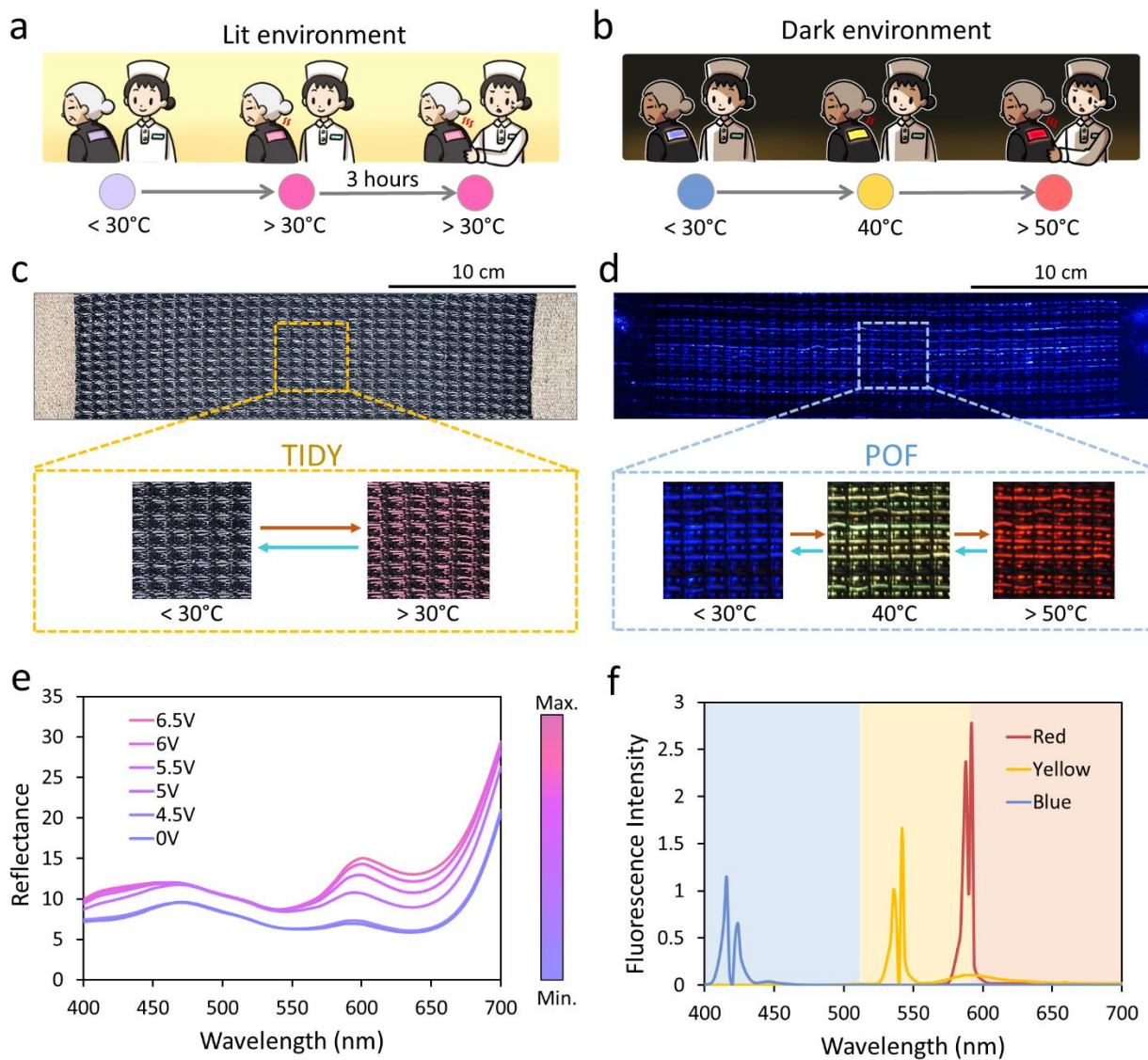


Fig. 3. Illuminative characterization of POE and TIDY. Schematic illustrations of colour change of (a) TIDY in lit environment and (b) POE in dark environment during application. Images of WIHF showing (c) heat-induced colour change in TIDY and (d) programmed colour change in POE. Wavelength of colour spectrum for (e) TIDY and (f) POE in terms of reflectance and fluorescence intensity respectively.

### Mechanical Properties

Traditional woven POE textiles are stiff,<sup>55</sup> limiting their application in wearables and clothing.

Therefore, this study conducted several tests to evaluate the surface and mechanical properties of this novel WIHF, which consists of conductive sliver-coated heating yarn, TIDY, and POF. Images and thermal images were captured for the fabric sample during twisting, bending, and shearing, respectively (see Fig. 4a, 4b, and 4c), demonstrating satisfactory flexibility and even distribution of heat during usage, even in heating mode.

The Kawabata Evaluation System (KES) was utilized for the mechanical evaluation of the fabric due to its advanced laboratory testing system for measuring the surface and mechanical properties of fabrics. In this study, the novel WIHF was compared not only to commercial woven POF but also to knitted POF textile with a soft hand feel proposed in recent years.<sup>55</sup> The images three POF fabric samples including commercial woven POF, knitted POF textile and illuminative heating POF textile in this work were shown in fig. S4. Table S3 presents the KES results for these three types of POF fabric in five categories: softness, flexibility, thermal insulation, surface smoothness, and stretchability. The overall results were converted into a radar figure (Fig. 4d), illustrating the superior surface and mechanical properties of WIHF compared to others in terms of softness, stretchability, and thermal insulation. Additionally, it exhibited excellent flexibility and surface smoothness comparable to knitted POF textile. The proposed WIHF exhibits significant improvements in hand feel and mechanical properties compared to traditional commercial woven POF textile, despite the illuminative heating textile possessing relatively high weight and thickness (Fig. S5a). In terms of tensile properties, WIHF in this work demonstrates the highest values in tensile energy (WT) and tensile recoverability (RT) as 9.4 g.cm/cm<sup>2</sup> and 57.8% respectively, indicating the greatest stretchability and recoverability than commercial woven POF fabric (6.7 g.cm/cm<sup>2</sup>, 53.5%) and knitted POF fabric (2.4 g.cm/cm<sup>2</sup>, 42.1%) (Fig. 4e). This result demonstrates that the hand feel of woven POF can be enhanced to match that of knitted structures. Regarding compression properties, the compressional linearity (LC) and compressional

energy (WC) of the textile in this study (1.15, 0.49 g.cm/cm<sup>2</sup>) are significantly greater than those of commercial woven POF (0.16, 0.05 g.cm/cm<sup>2</sup>). The compression properties of WIHF have improved as much as those of the knitted one (1.32 and 0.65 g.cm/cm<sup>2</sup>) (Fig. S5b). A value of LC closer to 1 indicates firmer compression, while a higher value in WC signifies higher compression susceptibility. Fig. 4f indicates surface properties among the three fabric samples. Higher values in 1/MMD indicate more smoothness and less roughness, while higher values in 1/SMD indicate more surface evenness. The results in this work (47.6, 0.12 $\mu$ m) and the knitted POF fabric (51.3, 0.13 $\mu$ m) are significantly greater than those of commercial woven POF fabric (25.7, 0.11 $\mu$ m).

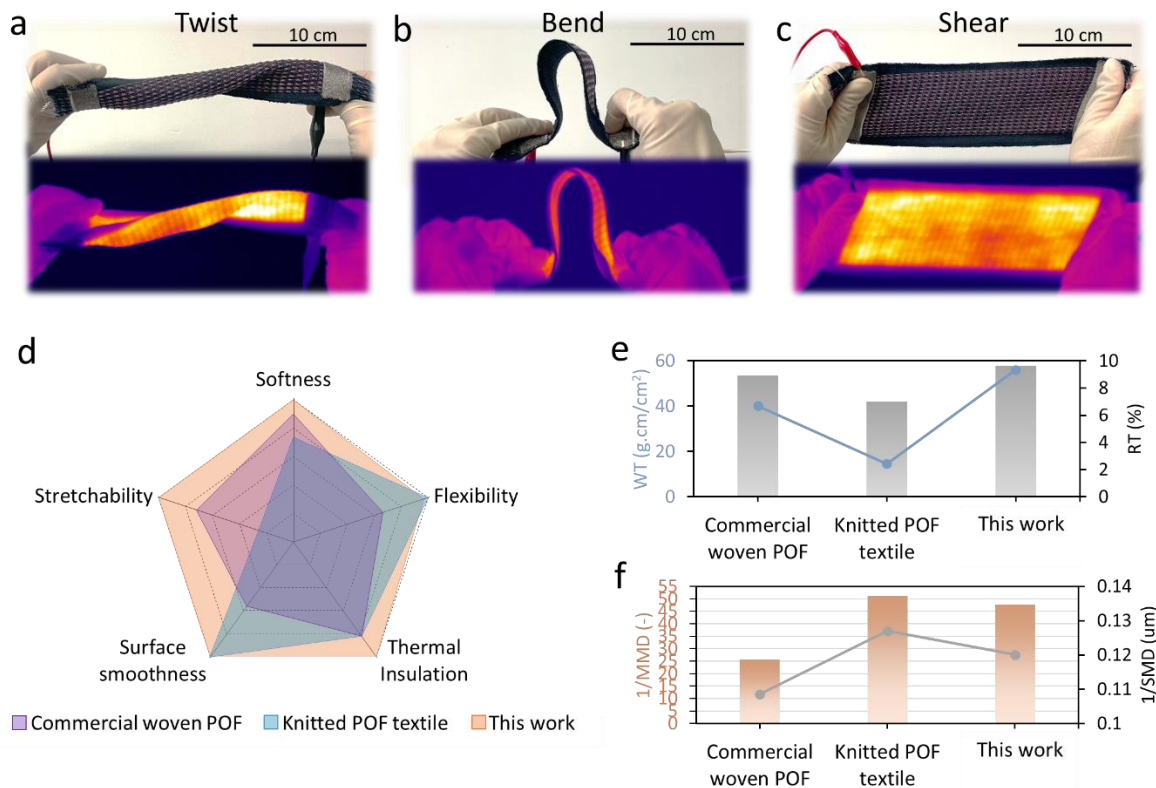


Fig. 4. Mechanical characterization of the WIHF. Images and thermal images of (a) twisting, (b) bending and (c) shearing the illuminative heating fabric. (d) Radar figure of mechanical properties of illuminative heating fabric. Comparison in (e) tensile properties and (f) surface properties of illuminative heating fabric and other POF fabrics.

## **ITHJ in Temperature Control**

A self-developed hardware with a micro-controller connecting WIHF to several electronic components to form ITHJ is shown in Fig. 5a. Prior to integrating the electrical components to create an all-in-one ITHJ, it was essential to train an ANN model to predict optimal thermal comfort for a diverse range of users. To achieve this, a process for collecting subject data was initiated to gather user information, including age, gender, height, and weight, as well as ambient parameters such as temperature, relative humidity, and air velocity. This data was utilized for deep learning in the self-training ANN model. The development process is illustrated in Fig. 5b.

A self-trained ANN model was developed by collecting data from 50 subjects aged between 18 and 89 to investigate the heating temperature required for optimal thermal comfort using ITHJ, considering variations in age, gender, height, and weight. The objective was to train the ANN model to predict the optimal heating temperature of the WIHF for users, thereby facilitating the attainment of maximum thermal comfort under varying ambient conditions. WIHF was positioned on the upper back torso of the jacket, as previous research has indicated this to be one of the effective positions for e-textiles to provide thermal comfort to users.<sup>28</sup> Fig. 5c shows the image of ITHJ which was fabricated by integrating several electronic components with WIHF. The indoor subject test setup is illustrated in Fig. 5d, where a fan was placed in front of the subject while they sat under the air conditioner. Two experimental cases, case 1 and case 2 were conducted. The preferred heating temperature for optimal thermal sensation from each subject was collected and is demonstrated in Fig. 5e. The results showed that all preferred heating temperatures fell within the testing temperature range of 40°C to 50°C, with the highest and most fluctuating preferences observed in the age group of 55-64. Thus, energy savings can be achieved by regulating and stabilizing the heating temperature between 40°C and 50°C for users of various ages, genders, and

body masses in both case 1 and case 2 conditions.

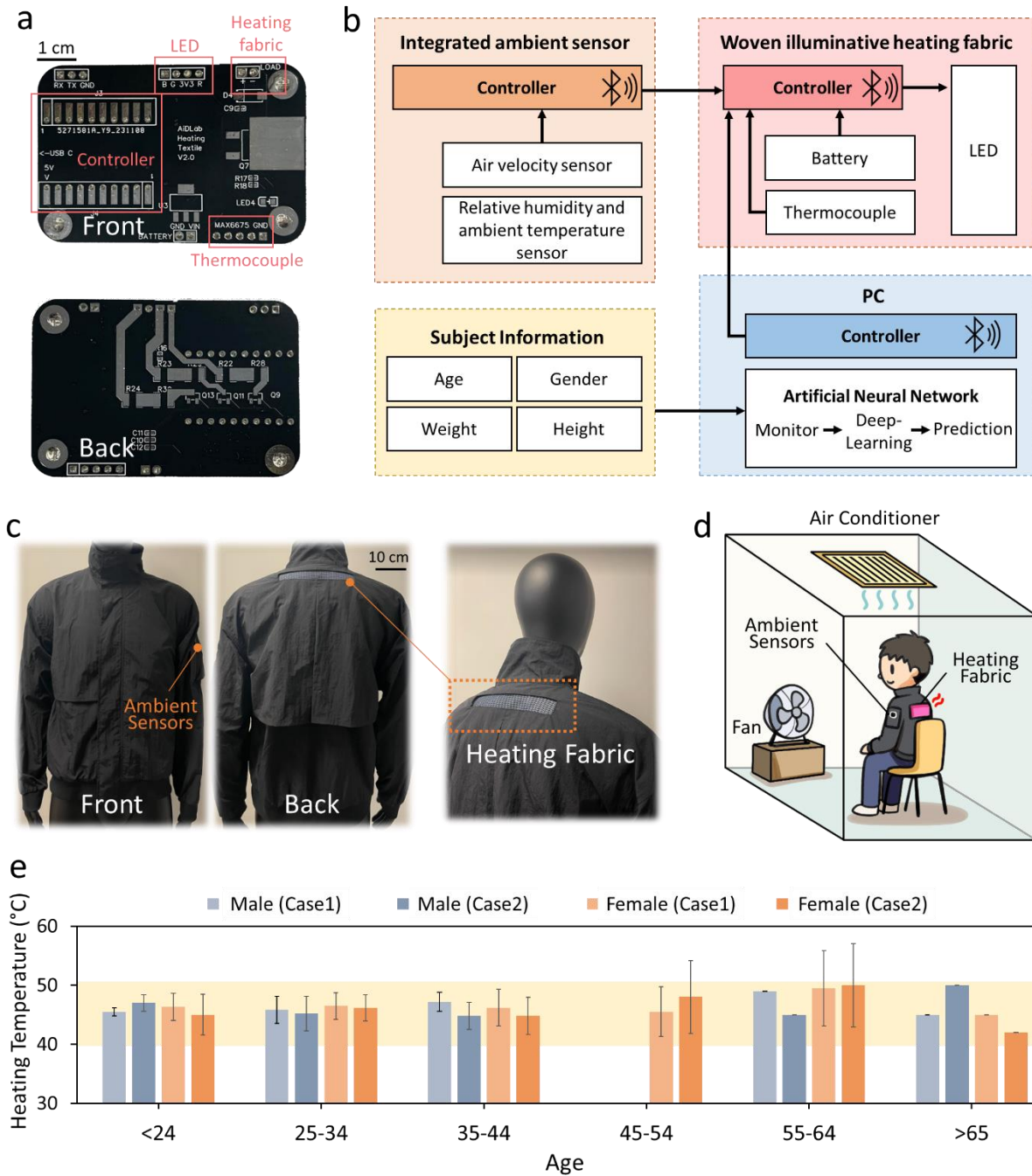


Fig. 5. Development of ITHJ. (a) Images of the self-developed multi-functional hardware. (b) Schematic illustration of development process. (c) Images of ITHJ. (d) Indoor subject test setting for data collection. (e) Comparison of heating temperature of jacket in achieving maximum

thermal comfort between female and male in different age groups.

The construction of the ANN model is illustrated in Fig. 6a. The input variables included subject information such as age (years), gender, height (cm), and weight (kg), as well as ambient parameters like temperature (°C), relative humidity (%RH), and air velocity (m/s). The target output variable was the heating temperature of the ITHJ to achieve maximum thermal comfort. The ANN model was trained using Python 3.12. A total of 100 datasets, shown in Table S4, were collected from subject tests to investigate various input parameters for achieving maximum thermal comfort in cases 1 and 2. During preprocessing, male was coded as "0" and female as "1". Eighty datasets were randomly selected for training the prediction model, while twenty datasets were used to test the accuracy of the ANN model in the final stage. Four hidden layers with 20 neurons each were incorporated into this ANN architecture to enhance its structural complexity with a substantial number of neurons. In the preliminary ANN model development, using sigmoid or ReLU activation functions, a comparison was conducted to find the configuration yielding the lowest MSE value, chosen as the error metric for higher predictive accuracy in this test.<sup>30</sup> MSE was used to evaluate the accuracy of predictions generated by the loss functions during ANN training. The computation of MSE is represented by the following equation:

$$MSE = \frac{\sum (y_i - \hat{y}_i)^2}{n} \quad (1)$$

where  $\hat{y}_i$  is the corresponding predicted value,  $y_i$  is the  $i^{th}$  observed value and  $n$  is the number of observations.

Alpha served as a regularization parameter to help prevent overfitting by penalizing large weights in the model. Due to underfitting with the default value of 0.0001, the final alpha applied was 1e-08. The initial learning rate was set to 1e-05. To achieve an optimal learning rate, the

learning rate was set to "adaptive," keeping it constant at the initial value as long as the training loss continued to decrease and to schedule weight updates accordingly. The solver "sgd" was used as the optimization algorithm to minimize the loss function during training by updating the model weights. This choice was made due to its suitability for large datasets and its ability to use momentum to accelerate convergence. After several epochs, the lowest MSE was achieved. Fig. 6b shows the number of neurons in the latest 50 epochs, with the least MSE at 5.083 using ReLU activation functions. The optimal configuration resulted in "1," "2," "5," and "1" neurons in hidden layers 1, 2, 3, and 4, respectively. The heating temperatures predicted by the ANN model for 20 actual datasets are shown in Fig. 6c. After running and validating the ANN model, the prediction model was integrated into the ITHJ for the final subject test. A 34-year-old male subject, 178 cm tall and weighing 74 kg, who did not participate in the initial data collection, was invited for the final subject test. The testing protocols were the same as in case 2. By increasing the heating temperature of the ITHJ by 1°C per minute, the highest comfort sensation was achieved at 47°C. In contrast, the ITHJ integrated with the ANN model maintained a constant heating temperature of  $47 \pm 0.5^\circ\text{C}$  and achieved a maximum comfort sensation rating of +3 (Fig. 6d). This demonstrates a high correlation between predicted and actual comfort levels.

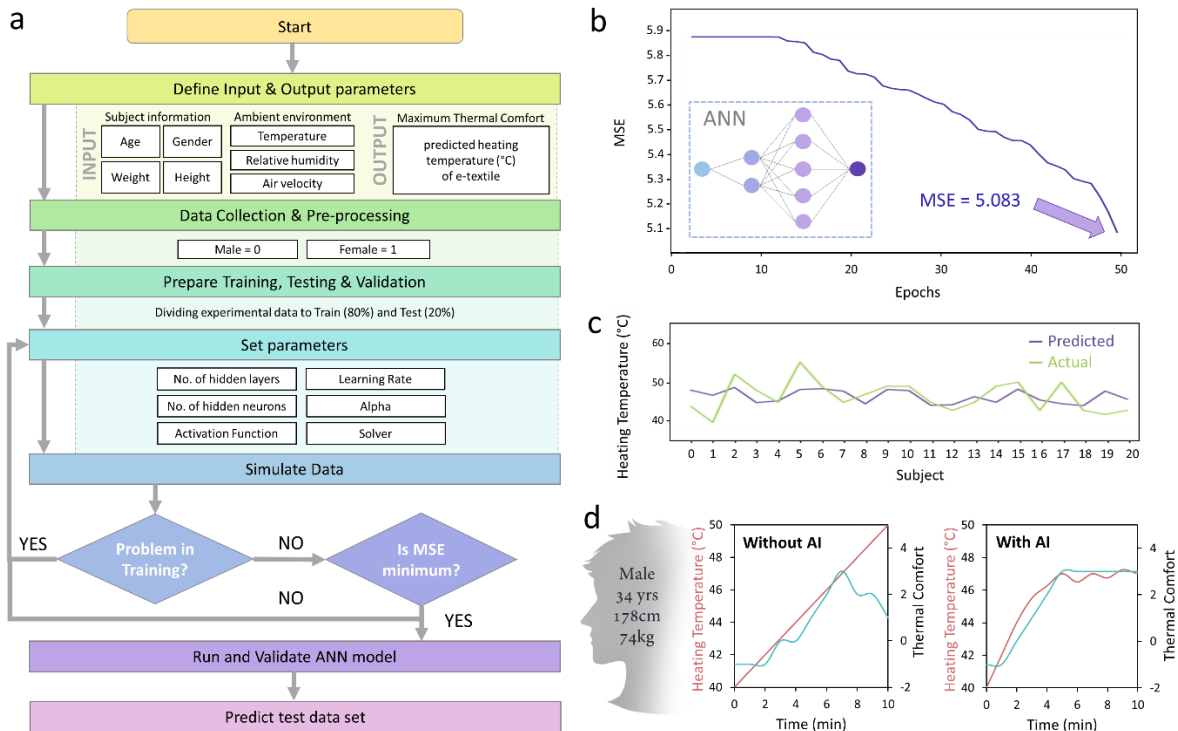


Fig. 6. ITHJ with ANN model in heating temperature prediction. (a) Flowchart of ANN construction. (b) Number of neurons in the latest 50 epochs with the least MSE. (c) Heating temperature predicted from ANN model to 20 actual datasets. (d) Comparison of heating temperature and comfort sensation of final subject test.

## CONCLUSION

In summary, WIHF was meticulously designed and developed to provide an excellent hand feel, characterized by softness, flexibility, elasticity, smoothness, and breathability. The fabric's thermochromic and illuminating effects, with superior brightness in both lit and dark environments, function as notifications to users and caregivers regarding prolonged heating duration. Future research will explore different weaving patterns and sizes to identify additional applications in wearable technology, furniture, and automotive sectors. Leveraging AI, the ITHJ has been developed to achieve automatic and intelligent temperature regulation, accounting for variables

such as the wearer's age, gender, weight, height, and ambient conditions including temperature, relative humidity, and air velocity, to maximize thermal comfort. This study represents an initial proof of concept with a limited dataset. To enhance the accuracy of the AI prediction model, larger sample sizes and more comprehensive datasets, encompassing a greater number of subjects and a variety of ambient parameter combinations, are necessary. The trained dataset from 50 wearability test subjects determined optimal heating temperatures (40-50°C) with a MSE of 5.083, demonstrating a high correlation between predicted and actual comfort levels in the final wear trial. The ITHJ concept effectively enhances thermal comfort and mitigates overheating risks, indicating its significant potential for wearable healthcare applications. By emphasizing structural development and functional integration, this work bridges the gap between material practicality and technological advancements, offering a novel approach for scalable applications.

## **MATERIALS AND METHODS**

### **Materials**

All textile materials used in this experiment are commercially available. The basic textile was 100% black cotton yarn with a specification of 40/2s, which is commonly available. TIDY, with a specification of 150D/2, was purchased from Shenzhen Xiancai Color Changing Technology Co., Ltd., China. POF, with a diameter of 0.25mm, was purchased from Mitsubishi Chemical Group Corporation, Japan. Two types of silver-coated yarns were used: one with a specification of 40D and electrical resistance of 32Ω/cm, purchased from Shandong Boyin Surface Functional Materials Co., Ltd., China, and another with a specification of 200D and electrical resistance of 2.54Ω/cm, purchased from Thinger Textile Co., Ltd., China.

### **Fabrication of WIHF**

In the weaving process, 40/2s black cotton yarn served as the passive warp yarn, while 40D silver-coated conductive heating yarn, TIDY, and POF were utilized in the weft direction. The warp and weft densities were 72 ends/inch and 80 ends/inch, respectively. A rapier sample loom weaving machine, model CCI/SL7900 from CCI Tech Inc., Taiwan, was used in the weaving process. Additionally, 200D silver-coated yarn served as the electrodes and was embroidered onto the fabric surface in the warp direction. An embroidery machine, model "SAI" from Tajima Embroidery Machines Ltd., Japan, was used for the embroidery process, with the pattern "Tatami 30" and 2903 stitches. The heating principle of the illuminative heating e-textile in this study can be expressed using Ohm's laws, defined as

$$I = \frac{V}{R} \quad (1)$$

Where  $I$ ,  $V$  and  $R$  correspond to current, volts and resistance respectively.<sup>56</sup> The power connection design of WIHF is simply made by connecting a pair of small buttons (Fig. S6), which prevents any discomfort after wearing. To achieve colour changing via illuminative POF, a programmed colour controlling system was applied to control the illumination of POF, including electronic components such as MOSFET, R1, R2, R3, and RGB colour modules (Fig. S7).

### **Fabrication of ITHJ**

The electronic components in ITHJ are connected as follows: The programmed LED colour control system of POF from Fig. S7, and the heating temperature control system from Fig. 2a, and the embedded thermocouple module set from Fig. S8, are all integrated into a self-developed hardware with a micro-controller which is shown in Fig. 5a. The real-time ambient sensor from Fig. S9 was connected via Bluetooth. The Bluetooth connection facilitates real-time remote temperature control and monitoring of the heating textile via a PC (Fig. S10). An integrated ambient sensor is

developed by combining an Arduino ESP32 microcontroller with a BME680 temperature, humidity, pressure, and gas sensor module, along with a Sparkfun FS3000 air velocity sensor module (Fig. S9) The Bluetooth connection of this integrated sensor facilitates good wireless signal quality, enabling the collection of ambient data and monitoring during experiments. Fig. S8 illustrates the schematic and photograph of the embedded temperature sensor on ITHJ, which serves as a thermocouple. The MAX6675 module is responsible for conducting cold-junction compensation and digitizing the signal obtained from a type-K thermocouple. Electric wires are connected on the edge of the embroidered WIHF to a microcontroller (ESP-32) and a power battery (+VIN) with a maximum 15V power supply. Electronic components including resistors (R1, R2, and R3), capacitor (C1), diodes (D), Metal-Oxide-Semiconductor Field-Effect Transistor (MOSFET), and LED are included in the electrical diagram. The LED light serves to indicate that the connection is working normally (Fig. 2a).

### **Characterization and Measurement**

The SEM images were taken by a tabletop microscope (model Hitachi TM3000). Microscopic views were taken by stereo microscope (model Leica M165 C). Colour-Eye Spectrophotometer (model 7000A, X-RITE GRETAG MACBETH) was applied to study reflectance at different power voltage supplies of TIDY. Spectrofluorometer (model FS5, Edinburgh Instruments Ltd) was applied in measuring fluorescence intensity of blue, yellow, and red illuminated colour of POF. Thermal images were captured by thermal image camera (Ti32, FLUKE). To evaluate heating efficiency, a multimeter was employed to measure fabric resistance under various power supplies. Thermometer equipped with thermocouples was used measure the heating temperature of fabric surface. Anemometer (DLX-ANE2302, DELIXI) was used to measure the air velocity.

KES was utilized for the mechanical properties measurement of WIHF in five categories:

softness, flexibility, thermal insulation, surface smoothness, and stretchability. Softness ( $S$ ) was tested by KES-FB3-A Compression Tester. It was calculated as

$$S = \frac{W}{T} \quad (2)$$

where  $W$  and  $T$  refer to weight and thickness. It represents the ratio of weight per unit area to thickness, indicating the nominal specific gravity of the fabric. A higher value suggests that the fabric contains more air and has a softer hand feel. Flexibility ( $F$ ) was tested by KES-FB2 Pure Bending Tester. The bending length can be expressed as

$$F = 1/\sqrt[3]{B/W} \quad (3)$$

where  $B$  and  $W$  refer to flexural rigidity and weight. This value indicates the distance that the fabric droops under its own weight. It reflects the fabric's bending length when bent at a consistent angle by its own weight and is named accordingly. As the value rises, the fabric becomes more resistant to bending, resulting in a higher draping coefficient. Regarding to thermal insulation, KES-F7 Thermo Labo was applied in testing. Higher values suggest better heat retention properties. Surface smoothness ( $SS$ ) was obtained by KES-FB4-A Friction Tester and it could be calculated using the equation

$$SS = 1\left(\frac{MMD}{SMD}\right) \quad (4)$$

where  $MMD$  and  $SMD$  refer to fluctuation of mean frictional coefficient and surface roughness.  $MMD/SMD$  represents the ratio of change  $MMD$  in coefficient of friction to surface roughness  $SMD$ . A smaller value indicates a smoother surface texture perceived by touch. This value is closely related to the tactile feel of the surface. Lastly, stretchability was obtained by KES-FB1 Tensile and Shear Tester. It is quantified as tensile energy ( $WT$ ), where higher values indicate greater stretchability.

## **Subject test**

Fifty healthy subjects were recruited for the study. Demographic information is provided in Table S5. Ethical approval was obtained from the University's Ethical Committee (HSEARS20200123003). All Participants avoided alcohol and strenuous exercise for 8 hours prior to the experiment. Additionally, they were instructed not to eat or drink coffee or tea for at least 3 hours before the test. Each subject wore a short-sleeved 100% cotton T-shirt before putting on the heating jacket in a cold environmental chamber under 21°C, 60%RH, 3m/s (case 1) and 17°C, 70%RH, 0m/s (case 2). The subject remained seated on a chair for 15 minutes prior to starting the wearer trial test. Following this acclimation period, the subject continued to remain seated as the heating power was activated. The heating temperature was gradually increased by 1°C per minute, from 40°C to 50°C over the course of 10 minutes. Data on ambient temperature (°C), relative humidity (%RH), air velocity (m/s), and the heating temperature (°C) required to achieve maximum thermal comfort were recorded for training the ANN model.

Based on findings from a previous study on heating e-textiles, which revealed significant effects on changes in mean skin temperature, thermal perception, and comfort perception ( $p < 0.05$ ) but no significant impact on metabolic rate or heart rate ( $p > 0.05$ ),<sup>28</sup> this study focused on recording heating temperature and skin temperature without considering metabolic rate or heart rate. In this study, skin temperature were measured using a thermocouple both before and after the test at the upper back position. Test would be started when the skin temperature ranged from 35 to 37°C. Evaluations were performed every minute using a Semantic Differential Scale for comfort sensation (-3 to +3).

## **SUPPORTING INFORTMATION**

This PDF file includes:

Figs. S1 to S10

Tables S1 to S5

Movies S1

## ACKNOWLEDGEMENTS

We appreciate the valuable technical support and advice from Ng, S. W. and Lee, C. H. on the specimen weaving process and the operation of the spectrophotometer and spectrofluorometer.

**Funding:** This research is funded by the Laboratory for Artificial Intelligence in Design (Project Code: RP3-5) under InnoHK Research Clusters, Hong Kong Special Administrative Region.

**Author contributions:** Lee, C., Tan, J. and Tan, J. J. conceived the idea and designed the experiments. Lee, C. and Tang, H. T. prepared woven and knitted POF textile samples. Tan, J. J. constructed the ANN model development. Lee, C. executed all the experiments and analysis. Yu, W. S. performed the pattern design of jacket. Lam, N. Y. K. conducted background research. All authors discussed the results and contributed to the manuscript. Tan, J. oversaw the project, revised the manuscript, and led the effort to completion.

**Competing interests:** Lee, C., Tan, J. and Tan, J. J. are inventors of a provisional patent filed in the China Patent on 10 October 2023, with Filing No. 2023113052662 (Chinese Patent No. 2308943HK01). The authors declare that they have no competing interests.

**Data and materials availability:** All data needed to evaluate the conclusions in the paper are present in the paper and/or the Supplementary Materials.

## REFERENCES

1. Šahta, I. , Baltina, I. , Truskovska, N. , Blums, J. , and Deksnis, E. , "Selection of conductive yarns for knitting an electrical heating element," *WIT Trans. Built Environ*, vol. 137, pp. 91-102, 2014.

2. Hao, L. , Yi, Z. , Li, C. , Li, X. , Yuxiu, W. , and Yan, G. , "Development and characterization of flexible heating fabric based on conductive filaments," *Measurement*, vol. 45, no. 7, pp. 1855-1865, 2012.
3. Hamdani, S. T. A. , Potluri, P. , and Fernando, A. , "Thermo-mechanical behavior of textile heating fabric based on silver coated polymeric yarn," *Materials*, vol. 6, no. 3, pp. 1072-1089, 2013.
4. Bahadir, S. K. , and Sahin, U. K. , "A wearable heating system with a controllable e-textile-based thermal panel," *Wearable Technol*, vol. 175, 2018.
5. Hasan, M. , Offermann, M. , Haupt, M. , Nocke, A. , and Cherif, C. , "Carbon filament yarn-based hybrid yarn for the heating of textile-reinforced concrete," *Journal of Industrial Textiles*, vol. 44, no. 2, pp. 183-197, 2014.
6. Luo, Y. W. , "Temperature adjusting and controlling pad," China Patent. (2016, Aug 31). *CN104013243A*. Accessed on: May. 1, 2024. [Online]. Available: <https://patents.google.com/patent/CN104013243A/en?q=CN104013243A>
7. Cheng, Q. , "Medical temperature rising blanket," China Patent. (2016, Feb 3). *CN205007104U*. Accessed on: May. 1, 2024. [Online]. Available: <https://patents.google.com/patent/CN205007104U/en>
8. Ellis, K. D. , "Device and Method for Temperature Management of Heating Pad Systems," Australia Patent. (2014, May 8). *AU2008224637B2*. Accessed on: May. 1, 2024. [Online]. Available: <https://patents.google.com/patent/AU2008224637B2/ko>
9. Chen, S. R. , Huo, Y. Z. , and Qiu, W. J. , "Controllable shoulder pad of medical temperature," China Patent. (2016, Sept 14). *CN205567912U*. Accessed on: May. 1, 2024. [Online]. Available: <https://patents.google.com/patent/CN205567912U/en>
10. Lin, G. , "Smart system and method for promoting sleep quality," China Patent. (2018, Apr 24). *CN105797270A*. Accessed on: May. 1, 2024. [Online]. Available: <https://patents.google.com/patent/CN105797270A/en>
11. Huang, J. , Liu, Y. , Chen, W. Q. , Zhu, Y. S. , and Zhang, D. F. , "Intelligent electric heating scarf," China Patent. (2022, Dec 11). *CN202958932U*. Accessed on: May. 1, 2024. [Online]. Available: <https://patents.google.com/patent/CN202958932U/en>
12. Wang, H. , and Bao, J. , "Intelligent temperature-regulation garment," China Patent. (2010, Jul 28). *CN101785586A*. Accessed on: May. 1, 2024. [Online]. Available: <https://patents.google.com/patent/CN101785586A/en>
13. Tabor, J. , Chatterjee, K. , and Ghosh, T. K. , "Smart textile-based personal thermal comfort systems: current status and potential solutions," *Adv. Mater. Technol.*, vol. 5, no. 5, p. 1901155, 2020.
14. Zhu, X. Q. , "Intelligent controller of electric heater," China Patent. (2023, Dec 23).

- CN203687188U. Accessed on: May. 1, 2024. [Online]. Available: <https://patents.google.com/patent/CN203687188U/en>
15. West, A. C. , "Thermal warming blanket for patient temperature management," US Patent. (2019, Mar 22). US6078026A. Accessed on: May. 1, 2024. [Online]. Available: <https://patents.google.com/patent/US6078026A/en>
  16. Corona, S. , "Heat mat with thermostatic control," US Patent. (2017, Oct 3). US20160192442A1. Accessed on: May. 1, 2024. [Online]. Available: 2016. <https://patents.google.com/patent/US20160192442>
  17. Zuo, X. , Zhang, X. , Qu, L. , and Miao, J. , "Smart fibers and textiles for personal thermal management in emerging wearable applications," *Adv. Mater. Technol.*, vol. 8, no. 6, p. 2201137, 2023.
  18. Labour and Welfare Bureau HKSAR. 2022. "The shortage of personnel in the institution: an indisputable fact". Director's Blog. Apr 3, 2022. [https://www.lwb.gov.hk/tc/blog/post\\_03042022.html](https://www.lwb.gov.hk/tc/blog/post_03042022.html)
  19. Hong, T. C. , 2024. " Consumer Council Elderly Homes | Private basic monthly fees vary by more than 12 times, with a staff-to-resident ratio as low as 1:35." HK01, Apr 15, 2024. <https://www.hk01.com/%E7%A4%BE%E6%9C%83%E6%96%B0%E8%81%9E/1010284/%E6%B6%88%E5%A7%94%E6%9C%83%E5%AE%89%E8%80%81%E9%99%A2-%E7%A7%81%E7%87%9F%E5%9F%BA%E6%9C%AC%E6%9C%88%E8%B2%BB%E7%9B%B8%E5%B7%AE%E9%80%BE12%E5%80%8D-%E4%BA%BA%E6%89%8B%E6%AF%94%E4%BE%8B%E5%8F%83%E5%B7%AE1-35>
  20. Slater, F. and Rees, W. , "The protective value of clothing," *J TEXT I. Proc.*, vol. 37, no. 7, pp. P132-P153, 1946.
  21. Li, L. , Au, W.-M. , Ding, F. , Hua, T. , and Wong, K. S. , "Wearable electronic design: electrothermal properties of conductive knitted fabrics," *Text. Res. J.*, vol. 84, no. 5, pp. 477-487, 2014.
  22. Chowdhury, M. A. , Joshi, M. , and Butola, B. , "Photochromic and thermochromic colorants in textile applications," *J ENG FIBER FABR*, vol. 9, no. 1, p. 155892501400900113, 2014.
  23. Chen, A. , Tan, J. , Henry, P. , and Tao, X. , "The design and development of an illuminated polymeric optical fibre (POF) knitted garment," *J TEXT I*, vol. 111, no. 5, pp. 745-755, 2020.
  24. Ge, L. , and Tan, J. , "Development of three-dimensional effects and stretch for polymeric optical fiber (POF) textiles with double weave structure containing spandex," *J TEXT I*,

- vol. 112, no. 3, pp. 398-405, 2021.
25. Tan, J. , "Photonic fabrics for fashion and interior," in *Handbook of smart textiles*: Springer Singapore, 2015, pp. 1005-1033.
  26. J Tan, J. , Shao, L. , Lam, N. Y. K. , Toomey, A. , and Ge, L. , "Intelligent textiles: designing a gesture-controlled illuminated textile based on computer vision," *Text. Res. J*, vol. 92, no. 17-18, pp. 3034-3048, 2022.
  27. J Tan, *et al.*, "Evaluating the usability of a prototype gesture-controlled illuminative textile," *J TEXT I*, vol. 115, no. 3, pp. 350-356, 2024.
  28. Lee, C. , Tan, J. , Lam, N. Y. K. , Tang, H. T. , and Chan, H. H. , "The effectiveness of e-textiles in providing thermal comfort: A systematic review and meta-analysis," *Text. Res. J*, vol. 93, no. 7-8, pp. 1568-1586, 2023.
  29. Colley, M. , Hartwig, S. , Zeqiri, A. , Ropinski, T. , and Rukzio, E. , "AutoTherm: A Dataset and Ablation Study for Thermal Comfort Prediction in Vehicles," *arXiv preprint arXiv:2211.08257*, 2022.
  30. Lee, C. , Tan, J. , Tan, J. J. , Tang, H. T. , Yu, W. S. , and Lam, N. Y. K. , "Integrating Artificial Intelligence for Optimal Thermal Comfort: A Design Approach for Electric Heating Textiles Aligned with User Preferences," *Text. Res. J*. DOI: 10.1177/00405175241275620.
  31. Wu, Y. *et al.*, "Development of smart heating clothing for the elderly," *J TEXT I Journal*, vol. 113, no. 11, pp. 2358-2368, 2022.
  32. Wu, J.-X. , and Liao, Y.-C., "Self-regulated thermal comfort control for wearable heating device," *J. Taiwan Inst. Chem. Eng.*, vol. 121, pp. 74-80, 2021.
  33. Wang, F. , and Lee, H. , "Evaluation of an electrically heated vest (EHV) using a thermal manikin in cold environments," *Annals of occupational hygiene*, vol. 54, no. 1, pp. 117-124, 2010.
  34. Kiekens, P. , and Jayaraman, S., *Intelligent textiles and clothing for ballistic and NBC protection: technology at the cutting edge*. Springer Science & Business Media, 2012.
  35. Mondal, K., "Recent advances in soft E-textiles," *Inventions*, vol. 3, no. 2, p. 23, 2018.
  36. Wang, L. , and Loh, K. J. , "Wearable carbon nanotube-based fabric sensors for monitoring human physiological performance," *MATER STRUCT*, vol. 26, no. 5, p. 055018, 2017.
  37. Li, Y.-Q. , Huang, P. , Zhu, W.-B. , Fu, S.-Y. , Hu, N. , and Liao, K. , "Flexible wire-shaped strain sensor from cotton thread for human health and motion detection," *Sci. Rep.*, vol. 7, no. 1, p. 45013, 2017.
  38. Zhou, W. , *et al.* , "Enhancing thermal comfort prediction in high-speed trains through machine learning and physiological signals integration," *J. Therm. Biol.*, vol. 121, p. 103828, 2024.

39. Rewitz, K. , and Müller, D. , "Influence of gender, age and BMI on human physiological response and thermal sensation for transient indoor environments with displacement ventilation," *BUILD ENVIRON*, vol. 219, p. 109045, 2022.
40. Ismar, E. , Kurşun Bahadır, S. , Kalaoglu, F. , and Koncar, V., "Futuristic clothes: electronic textiles and wearable technologies," *GLOB CHALL*, vol. 4, no. 7, p. 1900092, 2020.
41. Bertuleit, K. , "Silver coated polyamide: a conductive fabric," *Journal of Coated Fabrics*, vol. 20, no. 3, pp. 211-215, 1991.
42. Wang, H. , Siddiqui, M. Q. , and Memon, H. , "Physical structure, properties and quality of cotton," *Cotton science and processing technology: Gene, ginning, garment and green recycling*, pp. 79-97, 2020.
43. Elmogahzy, Y. , and Farag, R. , "Tensile properties of cotton fibers: importance, research, and limitations," in *Handbook of properties of textile and technical fibres*: Elsevier, 2018, pp. 223-273.
44. *Knitwarm*. (2024), (available at <https://www.knitwarm.com>)
45. *FabRoc™ Heat Technology*. (2024), (available at <https://exo2.com/pages/heat-technology>)
46. Kayacan, O. , and Yazgan Bulgun, E. , "Heating behaviors of metallic textile structures," *INT J CLOTH SCI TECH*, vol. 21, no. 2/3, pp. 127-136, 2009.
47. Department of Health HKSAR" A man suffered severe burns and blisters on his calves after falling asleep with a hot water bottle.," Sky Post, Dec 18, 2023. <https://www.etnet.com.hk/www/tc/health/105924/%E4%BF%9D%E6%9A%96%E8%A6%81%E5%B0%8F%E5%BF%83%EF%BD%9C%E7%94%B7%E5%AD%90%E6%94%AC%E6%9A%96%E6%B0%B4%E8%A2%8B%E7%9E%93%E8%A6%BA%E5%B0%8F%E8%85%BF%E7%9A%AE%E8%86%9A%E9%81%AD%E7%87%99%E7%86%9F%EF%BC%81%E9%86%AB%E7%94%9F%EF%B8%B0%E5%88%87%E5%BF%8C%E5%81%9A%E5%91%A2%E4%BB%B6%E4%BA%8B%EF%BC%81%E6%9A%96%E6%B0%B4%E8%A2%8B%E6%B0%B4%E6%BA%AB%E3%80%81%E5%88%86%E9%87%8F%E6%87%89%E8%A9%B2%E5%B9%BE%E5%A4%9A%E5%85%88%E5%AE%89%E5%85%A8%EF%BC%9F>
48. Choi, T. Y. , " Shocking! Elderly Man Suffers Second-Degree Burns from Hot Pack in Cold Weather, Leaving 10 cm Scarring," *ctinews*, Dec 26, 2022. <https://ctinews.com/news/items/Z3WgX8vVaK>
49. Law, K. Y. , " A woman suffered severe burns and blisters on her feet after using a hot water bottle for warmth. Doctor: Temperatures between 44 to 55°C can gradually damage the dermis layer.," *HKET*, Dec 17, 2020. <https://topick.hket.com/article/2830878/%E3%80%90%E4%BD%8E%E6%BA%AB%E7%87%99%E5%82%B7%E3%80%91%E5%A5%B3%E5%AD%90%E7%94%A8%E7>

%86%B1%E6%B0%B4%E8%A2%8B%E5%8F%96%E6%9A%96%E9%9B%99%E8%85%B3%E8%A2%AB%E4%BD%8E%E6%BA%AB%E7%87%99%E5%82%B7%E6%BD%B0%E7%88%9B%E3%80%80%E9%86%AB%E7%94%9F%EF%BC%9A44%E8%87%B355%C2%B0C%E5%8F%AF%E5%B0%8D%E7%9C%9F%E7%9A%AE%E5%B1%A4%E9%80%A0%E6%88%90%E6%BC%B8%E9%80%B2%E6%90%8D%E5%AE%B3

50. Chan, Y. W. , " The elderly woman suffered blisters from burns after placing a warm pack on the soles of her feet and sleeping with socks on.," CNA, Feb 1, 2021. <https://www.cna.com.tw/news/ahel/202102010225.aspx>
51. Ko, K. Y. , "Dr. Dōng: Prolonged use of heat packs increases the risk of "low-temperature burns"—be cautious of abdominal heatstroke.," on.cc, Dec 25, 2017. [https://hk.on.cc/hk/bkn/cnt/news/20171225/bkn-20171225063039322-1225\\_00822\\_001.html](https://hk.on.cc/hk/bkn/cnt/news/20171225/bkn-20171225063039322-1225_00822_001.html)
52. Lam, K. M. , "Heat packs and warmers provide warmth but can lead to "low-temperature burns." Dermatologists warn they may cause blisters and scarring—avoid using them while sleeping," mingpao, Dec 2, 2022. <https://news.mingpao.com/ins/%E7%86%B1%E9%BB%9E/article/20221202/s00024/1669792468440/%E6%9A%96%E5%8C%85%E6%9A%96%E8%A2%8B%E4%BF%9D%E6%9A%96%E9%98%B2%E3%80%8C%E4%BD%8E%E6%BA%AB%E7%87%99%E5%82%B7%E3%80%8D-%E7%9A%AE%E8%86%9A%E7%A7%91%E9%86%AB%E7%94%9F%E6%8F%90%E9%86%92%E5%8F%AF%E8%87%B4%E5%87%BA%E6%B0%B4%E6%B3%A1%E7%95%99%E7%96%A4-%E7%9D%A1%E8%A6%BA%E9%81%BF%E5%85%8D%E7%94%A8>
53. Lee, C. , Tan, J. , and Tan, J. J. , "Smart Textile," China, 2023. China Patent. (2023, Oct 10). 2308943HK01.
54. Zhao, Y. , "Study and development of novel thermal functional textile with conductive materials,"thesis, The Hong Kong Polytechnic University, Hong Kong. (2019).
55. Tan, J. , 2024. "Intelligent Textile System for Interiors, Fashion and Rehabilitation." AiD Lab, 4 Jul, 2024. <https://www.aidlab.hk/en/research/32>
56. Roh, J.-S. , and Kim, S. , "All-fabric intelligent temperature regulation system for smart clothing applications," *J. Intel. Mat. Syst. Str.* vol. 27, no. 9, pp. 1165-1175, 2016.

For Table of Contents Only:

